Conventional data display and implications for the interpretation of seismic profiles: a discussion on the ViDEPI seismic database offshore Apulia (southern Italy)

Marianna Cicala[1], Domenico Chiarella[2], Francesco De Giosa[3], Vincenzo Festa[1]*

[1] Dipartimento di Scienze della Terra e Geoambientali, Università degli Studi di Bari "Aldo Moro", 70125 Bari, Italy.

[2] Clastic Sedimentology Investigation (CSI), Department of Earth Sciences, Royal Holloway, University of London, Egham, Surrey, TW20 0EX, UK

[3] Environmental Surveys S.r.l. (ENSU) – Spin-Off dell'Università degli Studi di Bari "Aldo Moro", 74123 Taranto, Italy

*Corresponding author. E-mail address: vincenzo.festa@uniba.it (V. Festa).

ABSTRACT

The present paper analyses old seismic profiles and exploration well logs, from the Marine Zones B, D and F (offshore the Apulia region, southern Italy), included in the Visibility of Petroleum Exploration Data in Italy (ViDEPI) project. The public seismic profiles available from this project present several limitations since basic information for an accurate geological interpretation are missing, such as the basic shape of the seismic wavelets and the seismic polarity. In this study, a review of the basic pulse shape and polarity of seismic wavelets, as well as the shape and polarity of principal reflectors has been addressed. With the purpose of revealing the shape and polarity of the seismic profiles from the Marine Zones B, D and F, the seismic pattern of the reflectors at the sea

floor has been analysed. Finally, lithostratigraphic and sonic logs have been used to identify abrupt interval velocity variations between different lithostratigraphic successions, resulting in a geological meaning of the principal reflectors.

Keywords

Wavelet shape, wavelet polarity, ViDEPI project, offshore Apulia, interpretation of seismic lines

Declaration of competing interest

The authors declare that they have no known competing financial interests or personal relationships that could have appeared to influence the work reported in this paper.

Introduction

The Visibility of Petroleum Exploration Data in Italy (ViDEPI) project is the most complete and public database of technical documents related to hydrocarbon exploration in Italy. The project contains data dated back to the 1957, held by the Ministry for the Economic Development of the Italian Government. As far as we know, it is one of the largest public database in the Mediterranean area which includes seismic profiles and exploration well logs. The database is accessible since 2007 on www.videpi.com, from which documents in PDF format can be downloaded. The seismic profiles located offshore the Italian Peninsula (Fig. 1a) have been divided into seven Marine Zones named from A to G. In particular, the dataset used and discussed in this study is located offshore the Apulia region pertaining to the Marine Zones B, D and F (Fig. 1b).

The seismic profiles falling in the Marine Zones B and D were acquired in the late ‘60s, whereas the ones within the Marine Zone F are dated back to the mid-‘70s of the last century. In the recent years, several research papers benefitted from the release of these subsurface data focusing on the Mesozoic Apulia Platform and adjacent basins rooted on the Adria plate, that were tectonically involved, during Cenozoic, in the Dinarides-Hellenides (to the East) and Apennines (to the West) orogenic deformations (Fig. 1a and 1c) (Antoncecchi et al. 2013; Scisciani and Calamita 2009; Cicala et al. 2021; Del Ben et al. 2008, 2010, 2015; Festa et al. 2014, 2019a, b; Finetti and Del Ben 2005; Maesano et al. 2020; Milia et al. 2017a, b; Nicolai and Gambini 2007; Pace et al. 2015; Santantonio et al. 2013; Teofilo et al. 2016, 2018; Tropeano et al. 2013; Volpi et al. 2015, 2017).

However, seismic data available from the ViDEPI project present several limitations since they underwent to a preliminary processing standard sequence procedure (Yilmaz 2001), resulting in unmigrated seismic profiles lacking basic information for an accurate geological interpretation. The basic shape of the seismic wavelets and the seismic polarity are missing in the seismic profile headers. Moreover, the visualization of the single pulse is very difficult due to the low resolution of the graphic rendering, as well as to the poor processing of the seismic data. Nevertheless, reflectors are quite clearly visible in several cases, giving the possibility to make considerations on the polarity of the seismic wavelets. Consequently, the seismic wavelets polarity allows to interpret correctly, as much as possible, the position of geological boundaries.

Aim of the present contribution is to detect the shape and polarity and geological meaning of the principal reflectors visible within the seismic profiles available in the Marine Zones B, D and F. To reach this aim, lithostratigraphic and sonic logs were used to identify abrupt interval velocity variations between different lithostratigraphic successions.

Basic pulse shape and polarity of seismic wavelets

The evaluation of the pulse shape represents a key step for seismic interpretation (e.g., Badley 1987; Veeken and van Moerkerken 2013). The seismic pulses displayed on seismic profiles are represented by two antithetic main types: (i) minimum-phase and (ii) zero-phase. The minimum-phase pulse consists of a succession of waves in a dumped sinusoidal trend, with the acoustic impedance boundary located at the wavelet onset (Fig. 2a-d). Conversely, the zero-phase pulse is characterised by a succession of waves arranged as a symmetrical dumped sinusoidal trend, i.e., lower amplitudes waves positioned aside of a central higher amplitude wave. The crest of this latter wave is interpreted to be the acoustic impedance boundary (Fig. 2e-h). It is important to keep in mind that the trough and peaks represent the wave positioned on left and right of the wiggle line respectively, and the area underneath the peak is conventionally filled in black (Fig. 2).

The wavelet polarity consists of a conventional representation of the abrupt variation of the reflection coefficient, and it conventionally changed over the time. According to the last standards proposed by the Society of Exploration Geophysicists (SEG) in the 2002, both normal and reverse polarities are defined under abrupt acoustic impedance increase with depth conditions. In particular, the normal polarity corresponds to (i) the onset of a trough if represented by the minimum-phase pulse (Fig. 2a), and (ii) to the higher peak if by the zero-phase pulse (Fig. 2e). Conversely, the reverse polarity corresponds to the onset of a peak (minimum-phase pulse) (Fig. 2b), or to the higher trough (zero-phase pulse) (Fig. 2f) (Sheriff 2002). However, in the North Sea and some other areas the convention for the zero-phase wavelet is reversed (Sheriff 2002; Veeken and van Moerkerken 2013), with the normal polarity corresponding to the higher trough (Fig. 2f), and the reverse polarity corresponding to the higher peak (Fig. 2e).

Similarly, considering an abrupt acoustic impedance decrease with depth, the normal polarity corresponds to the onset of a peak (minimum-phase pulse) (Fig. 2c), or to the higher trough (zero-phase pulse) (Fig. 2g) (e.g., Badley 1987). Accordingly, the reverse polarity would correspond to opposite situation (Figs. 2d and 2h).

It is important to point out that legacy seismic profiles, acquired before the last update of the SEG standards (Sheriff 2002), not always follow the same standards regarding the displaying of the polarity and the wavelet shape (Veeken and van Moerkerken 2013). To make everything more challenging, for legacy seismic profiles acquired in the Marine Zone B, D and F (ViDEPI 2021) (Fig. 1b) information about the polarity and the pulse shape are not available. Accordingly, the following issues, in terms of seismic interpretation, are present:

(i) minimum-phase normal polarity related to an abrupt increase of acoustic impedance with the depth (Fig. 2a) is equal to minimum-phase reverse polarity due to an abrupt decrease of acoustic impedance with the depth (Fig. 2d);

(ii) minimum-phase reverse polarity related to abrupt increase of acoustic impedance with the depth (Fig. 2b) is equal to minimum-phase normal polarity due to abrupt decrease of acoustic impedance with the depth (Fig. 2c);

(iii) zero-phase normal polarity related to abrupt increase of acoustic impedance with the depth (Fig. 2e) is equal to zero-phase reverse polarity due to abrupt decrease of acoustic impedance with the depth (Fig. 2h);

(iv) zero-phase reverse polarity related to abrupt increase of acoustic impedance with the depth (Fig. 2f) is equal to zero-phase normal polarity due to abrupt decrease of acoustic impedance with the depth (Fig. 2g).

Shape and polarity of principal reflectors applied to the seismic dataset

To clarify the display convention used for the wavelet shape and related polarity, the seismic pulse at the sea floor represents an unequivocal record since it is clearly related to an abrupt increase of the acoustic impedance with depth at the sea water/sea floor interface. The four reconstructed theoretical reflectors potentially expected at this interface are shown in figure 3. Because only one of these four possibilities represent the correct wavelet shape and polarity, it is important to have a scientific approach to coherently detect the right one. Our approach suggests that the comparison of the pattern of the reflectors visible in the seismic line with the reconstructed theoretical reflectors expected at the acoustic impedance boundary (Fig. 3) can help to recognize the correct wavelet shape and polarity.

If the proposed approach is applied to the legacy seismic lines used in this study (see Fig. 1b), it strongly suggests a zero-phase normal polarity (Fig. 3c) for seismic profiles acquired in the Marine Zone B (Fig. 4a). In particular, the zero-phase normal polarity is characterised by peaks strong reflector sided upward and downward by troughs (Figs 3c and 4a). Accordingly, the seafloor should be traced in the middle of the peaks strong reflector (Fig. 4a).

The analysis results a bit more difficult when applied to the seismic profiles of the Marine Zone D. Here, the displayed reflector pattern at the sea water/sea floor interface is comparable with both a zero-phase normal polarity (Fig. 4b) or a zero-phase reverse polarity (Fig. 4c). However, in some seismic profiles the zero-phase reverse polarity has been also observed like characterised by two strong reflectors, made up of peaks, separated by troughs (Figs 3d and 4c). Accordingly, the seafloor could be traced both in the middle of the strong peaks reflector (Fig. 4b), or in the middle of the troughs (Fig. 4c).

Finally, for the Marine Zone F seismic profiles the abrupt increase of acoustic impedance boundary (Fig. 3) suggests a zero-phase reverse polarity (Fig. 3d) (Figs 4d and 4e). The seafloor should be traced in the middle of the troughs (Fig. 4d and 4e).

The interpretation of seismic profiles must consider the wavelet shape and the polarity revealed by the reflectors dealing with the sea water/sea floor interface. The major abrupt variation of acoustic impedance with depth should comply with the reconstructed theoretical reflectors expected at the related interfaces. Therefore, in addition to the four cases shown in figure 3, the abrupt decrease of acoustic impedance with depth is reconstructed in the four frames of figure 5: two for the minimum-phase shape pulse (Fig. 5a, b) and two for the zero-phase wavelet (Fig. 5c, d). As of the old public seismic profiles of the Apulian B, D and F marine zones (ViDEPI 2021), the recognition of abrupt variations of acoustic impedance with depth should be restricted for the zero-phase wavelet (Fig. 3c, d, and Fig. 5c, d).

To investigate the response of geological boundaries in depth, exploration wells are used. The analysis of sonic logs available for some of the exploration wells present in the study area, i.e., Sabrina-1, Simona-1, Cristina-1, Branzino-1, Famoso-1, Chiara-1, Grazia-1, Grifone-1, Medusa-1, Giove-1-2 and Sparviero-1bis (Fig. 1b), allowed us to estimate the interval velocities for the Plio-Pleistocene clay-dominated interval, the Oligo-Miocene succession mainly composed of marls, marly limestones and calcarenites, and the Mesozoic-Eocene platform limestones or basin cherty limestones (Fig. 1c). Operatively, and according to Rider (2002), an average value for each of the above intervals of the interval transit time Δt has been graphically obtained from the sonic log; the unit of Δt is μs/ft, where μs is microseconds and ft is feet. In the example of figure 6, regarding the Giove1-2 exploration wells, $\Delta t = 158$ μs/ft and $\Delta t = 68$ μs/ft have been obtained for the Plio-Pleistocene clay-dominated interval and Oligo-Miocene succession mainly composed

of calcarenites, respectively. Successively, the interval velocity 1/Δt has been obtained, and converted into the metric velocity m/s (m = meters, s = seconds, μs = 10^{-6}s, ft = 0.3048 m) (Rider 2002). Therefore, the following interval velocities have been estimated: 1900-2500 m/s for the Plio-Pleistocene clay-dominated interval, 4800 m/s for the Messinian gypsum rocks of the Gessoso-Solfifera Fm, 2400-3900 m/s (exceptionally 4500 m/s in the Giove-1-2- exploration well) for the Oligo-Miocene succession mainly composed of marls, marly limestones and calcarenites, and 4900-6350 m/s for the Mesozoic-Eocene platform limestones or basin cherty limestones (Figs 1c and 7). It should be noted that the obtained velocities are comparable to those reported by Morelli (2002) and Teofilo et al. (2018) for the same lithotypes in the offshore the Apulia. Interval velocity abrupt increase corresponding to an abrupt increase of the acoustic impedance have been thus identified. Unfortunately, due to the low definition of the graphic rendering and the poor processing of the seismic data the reflectors related to this interval velocity abrupt variations are not always clearly visible. However, they can be recognised with peculiar characteristics.

From the top, the first important recognised variation of velocity with the depth consists of an abrupt increase (e.g., Fig. 6), which we can use to identify the key stratigraphic boundary between the Plio-Pleistocene succession and the underlying Messinian or Oligo-Miocene intervals. For the marine zones D and F, the correlation between exploration wells Grazia-1, Giove-1-2, and Medusa-1 and the seismic lines D-453, F76-16, and F76-33, respectively (Fig. 1b), shows the Plio-Pleistocene/Oligo-Miocene interface represented by strong troughs characteristically sided upward and downward by peaks reflectors (Figs 3c and 7a-c). This seismic response is in line with the zero-phase reverse polarity shown by the reflectors dealing with the sea water/sea floor interface (Figs 7a-c).

The Oligo-Miocene succession is locally topped by the Messinian Gessoso-Solfifera Fm dominated by gypsum rocks, and up to 110 m thick (Famoso-1 exploration well) (Fig. 7d). The database of the Marine Zone B is suitable for the investigation of the seismic response to this interface, given the possible correlation between seismic profiles and Sabrina-1, Simona-1, Branzino-1, Famoso-1 exploration wells (Fig. 1b, for their location). Because for the seismic profiles acquired within the Marine Zone B the zero-phase normal polarity has been deduced (e.g., Figs 4a and 7d), the Plio-Pleistocene clays/Gessoso-Solfifera Fm contact should be represented by a strong peaks reflector (Figs 3c and 7d). Deeper, the subsequent abrupt decrease of the velocity consists of the transition between the Gessoso-Solfifera Fm and the underlying Miocene marls and marly limestones deposits (Fig. 7d). However, the expected seismic response to this velocity change (e.g., Fig. 5c) is often seismically undetected due to the typical reduced thickness (decametric order) of the Miocene succession when topped by the Gessoso-Solfifera Fm.

An additional key easily recognisable in seismic line is the transition to the Mesozoic-Eocene platform and basins deposits characterised by the higher interval velocity (Fig. 1c). In particular, the abrupt increase of interval velocity from Oligo-Miocene succession and Mesozoic-Eocene basin carbonates can be extrapolated from the sonic logs of the Grazia-1 and Grifone-1 exploration wells (Fig. 1b). The seismic response of this transition can be observed on seismic profiles D-453 and F76-19, crosscutting Grazia-1 and Grifone-1 exploration wells, respectively, and characterised by zero-phase reverse polarity deduced by the pattern of reflectors dealing with the sea water/sea floor interface (Figs 7a and 7e). Accordingly, the top of the Mesozoic-Eocene basinal carbonates is seismically expressed by strong troughs sided upward and downward by peaks reflectors (e.g., Fig. 3d), as visible in the seismic profiles D-453 (Fig. 7a) and F76-19 (Fig. 7e). Similarly to the top of basinal deposits, the top of the Mesozoic-Eocene platform carbonates is represented by strong troughs sided upward and downward by peaks

reflectors (e.g., Figs 3d and 7c), as shown by the correlation between the Medusa-1 exploration well and the seismic line F76-33 (Fig. 1b). This seismic reflection pattern is conforming to the zero-phase reverse polarity exhibited by the reflectors characterising the sea water/sea floor interface (Fig. 7c). Finally, the abrupt increase of interval velocity due to the presence of the Mesozoic-Eocene platform carbonates can be assumed also by the sonic logs of Simona-1, Sabrina-1, Chiara-1 and Famoso-1 exploration wells (Fig. 1b, for the location). Unfortunately, Chiara-1 exploration well can't be correlated to the nearest seismic profile (B Marine Zone) due to too much distance between them. Again, in the seismic profiles crosscutting Simona-1, Sabrina-1 and Famoso-1 exploration wells, the seismic response of the Gessoso-Solfifera Fm, with a reduced thickness, masks the reflection of the underlying top of the Mesozoic-Eocene platform carbonates.

Since the range of the estimated velocity is quite large for each seismostratigraphic unit, and because several reflectors could be present in the related depth ranges, it is important to take into consideration the interpretation made on larger parts of the seismic profiles (e.g., Fig. 7) to identify unconformities as reflectors/boundaries of that units.

Concluding remarks

The analysis of the seismic profiles from the Marine Zones B, D and F, and of the stratigraphic and sonic logs of exploration wells, located offshore the Apulia region, support the following main conclusions:

(i) in order to detect the display of both the wavelet shape and the polarity, the seismic pulse at the sea floor represents an unequivocal record since it is clearly related to an abrupt increase of the acoustic impedance with depth at the sea water/sea floor interface. Accordingly, the comparison of the pattern of the reflectors visible in the seismic line with

the reconstructed theoretical reflectors expected at the acoustic impedance boundary can help to recognize the correct wavelet shape and polarity;

(ii) a zero-phase normal polarity has been revealed for the seismic profiles acquired in the Marine Zone B. The revelation of the basic shape of the seismic wavelets and the seismic polarity results a bit more difficult for the seismic profiles of the Marine Zone D. The displayed reflector pattern at the sea water/sea floor interface is comparable with both a zero-phase normal polarity or a zero-phase reverse polarity. Accordingly, an accurate analysis of the seismic pulse at the sea floor should be made for each seismic profile of the Marine Zone D. Finally, a zero-phase reverse polarity have been revealed for the Marine Zone F seismic profiles;

(iii) the analysis of sonic logs available for some of the exploration wells allowed us to obtain the interval velocities for: the Plio-Pleistocene clay-dominated interval, i.e., 1900-2500 m/s, the Messinian gypsum rocks of the Gessoso-Solfifera Fm, i.e., 4800 m/s, the Oligo-Miocene succession mainly composed of marls, marly limestones and calcarenites, i.e., 2400-3900 m/s and exceptionally 4500 m/s, and the Mesozoic-Eocene platform limestones or basin cherty limestones, i.e., 4900-6350 m/s;

(iv) despite the low definition of the graphic rendering and the poor processing of the seismic data, the reflectors related to interval velocity abrupt variations can be recognised with the peculiar characteristics depending on the basic shape of the seismic wavelets and the seismic polarity of the seismic profiles.

Acknowledgements

We are grateful to Alfonsa Milia and François Roure, whose suggestions helped us to improve the manuscript. MC thanks the PhD in Geosciences grant of the Università degli

Studi di Bari Aldo Moro. VF thanks the “Fondo per le Attività Base di Ricerca – 2017” grant and the “Convenzione tra Autorità di Bacino della Puglia e Dipartimento Geomineralogico dell’Università degli Studi di Bari per studi petrografici e mineralogici, oltre che geologico-strutturali, nell’area di Lesina Marina (FG)—2009” research funds.

References

Antoncecchi I, Teofilo G, Tropeano M, Festa V, Sabato L (2013) Platform-vs shelf-margins in Apulia (southern Italy). J Mediterr Earth Sci, Special issue 1, 13

Badley M E (1987) Practical Seismic Interpretation. International Human Resources Development Corp., Boston, Massachusetts, USA

Cicala M, Festa V, Sabato L, Tropeano M, Doglioni C (2021) Interference between Apennines and Hellenides foreland basins around the Apulian swell (Italy and Greece). Mar Pet Geol 133, 105300. https://doi.org/10.1016/j.marpetgeo.2021.105300

de Alteriis G (1995) Different foreland basins in Italy: examples from the central and southern Adriatic Sea. Tectonophysics 252, 349–373. https://doi.org/10.1016/0040-1951(95)00155-7

Del Ben A, Barnaba C, Taboga A (2008) Strike-slip systems as the main tectonic features in the Plio-Quaternary kinematics of the Calabrian Arc. Mar Geophys Res 29, 1–12. https://doi.org/10.1007/s11001-007-9041-6

Del Ben A, Geletti R, Mocnik A (2010) Relation between recent tectonics and inherited Mesozoic structures of the central-southern Adria plate. Boll Geofis Teor Appl, 51, 99–115

Del Ben A, Mocnik A, Volpi V, Karvelis P (2015). Old domains in the South Adria plate and their relationship with the West Hellenic front. J Geodyn 89, 15–28. https://doi.org/10.1016/j.jog.2015.06.003

Fantoni R, Franciosi R (2010). Tectono-sedimentary setting of Po Plain and Adriatic foreland. Rend Lincei-Sci Fis, 21/1, 197–209. https://doi.org/10.1007/s12210- 010-0102-4

Festa V, De Giosa F, Moretti M, Del Gaudio V, Pierri P (2019) In search of the seismogenic fault of the March 23rd 2018 earthquake (Mw 3.7) near Brindisi (Puglia, Southern Italy). Geol Croat 72, 137–144. https://doi.org/10.4154/gc.2019.10

Festa V, Fregola R A, Acquafredda P, De Giosa F, Monno A, Ventruti G (2019) The enigmatic ascent of Ca-sulphate rocks from a deep dense source layer: evidences of hydration diapirism in the Lesina Marina area (Apulia, southern Italy). Int J Earth Sci 108, 1897–1912. https://doi.org/10.1007/s00531-019-01739-1

Festa V, Teofilo G, Tropeano M, Sabato L, Spalluto L (2014) New insights on diapirism in the Adriatic sea: The Tremiti salt structure (Apulia offshore, Southeastern Italy). Terra Nova 26, 169–178. https://doi.org/10.1111/ter.12082

Finetti I R, Del Ben A (2005) Crustal Tectono-Stratigraphic Setting of the Adriatic Sea, in: Finetti, I.R. (Ed.), CROP PROJECT: Deep Seismic Exploration of the Central Mediterranean and Italy. pp. 519–547

Google Earth Pro (2021) Google LLC.

Maesano F E, Volpi V, Civile D, Basili R, Conti A, Tiberti M M, Accettella D, Conte R, Zgur F, Rossi G (2020) Active Extension in a Foreland Trapped Between Two Contractional Chains: The South Apulia Fault System (SAFS). Tectonics 39. https://doi.org/10.1029/2020TC006116

Milia A, Iannace P, Torrente M M (2017a) Active tectonic structures and submarine landslides offshore southern Apulia (Italy): A new scenario for the 1743 earthquake and subsequent tsunami. Geo-Marine Lett 37, 229–239. https://doi.org/10.1007/s00367-017-0493-7

Milia A, Torrente M M, Iannace P (2017b) Pliocene-Quaternary orogenic systems in Central Mediterranean: The Apulia-Southern Apennines-Tyrrhenian Sea example. Tectonics 36, 1614–1632. https://doi.org/10.1002/2017TC004571

Morelli D (2002) Evoluzione tettonico-stratigrafica del Margine Adriatico compreso tra il Promontorio garganico e Brindisi. Mem Soc Geol It., 57, 343-353

Nicolai C, Gambini R (2007) Structural architecture of the Adria platform-and-basin system. Boll Soc Geol Ital, Suppl. 7, 21–37

Pace P, Scisciani V, Calamita F, Butler R W H., Iacopini D, Esestime P, Hodgson N (2015) Inversion structures in a foreland domain: Seismic examples from the Italian Adriatic Sea. Interpretation 3, SAA161–SAA176. https://doi.org/10.1190/INT-2015-0013.1

Rider, M (2002) The geological interpretation of well logs, Whittles Publishing, Dunbeath, Caithness, Scotland, UK

Santantonio M, Scrocca D, Lipparini L (2013) The Ombrina-Rospo Plateau (Apulian Platform): Evolution of a Carbonate Platform and its Margins during the Jurassic and Cretaceous. Mar Pet Geol, 42, 4–29. https://doi.org/10.1016/j.marpetgeo.2012.11.008

Scisciani V, Calamita F (2009) Active intraplate deformation within Adria: Examples from the Adriatic region. Tectonophysics 476, 57-72

Sheriff R (2002) Encyclopedic dictionary of applied geophysics, Society of Exploration Geophysicists, Tulsa, Oklahoma, USA

Teofilo G, Antoncecchi I, Caputo R (2018) Neogene-Quaternary evolution of the offshore sector of the southern Apennines accrectionary wedge, Gulf of Taranto, Italy. Tectonophysics 378-379, 16-32. https://doi.org/10.1016/j.tecto.2018.05.006

Teofilo G, Festa V, Sabato L, Spalluto L, Tropeano M (2016) 3D modelling of the Tremiti salt diapir in the Gargano offshore (Adriatic Sea, southern Italy): constraints on the Tremiti Structure development. Ital J Geosci 135, 474-485. https://doi.org/10.3301/IJG.2015.40

Tropeano M, Festa V, Teofilo G, Sabato L, Spalluto L (2013) Stratigraphic constraints about timing of the Tremiti ridge uplift (offshore Apulia, southern Italy), J Mediterr Earth Sci, Special issue 1, 141-143

ViDEPI (2021), Visibilità dei dati afferenti all'attività di esplorazione petrolifera in Italia. https://www.videpi.com/

Veeken P, Moerkerken B (2013) Seismic Stratigraphy and Depositional Facies Models, EAGE Publications, Academic Press

Volpi V, Del Ben A, Civile D, Zgur F (2017) Neogene tectono-sedimentary interaction between the Calabrian Accretionary Wedge and the Apulian Foreland in the northern Ionian Sea. Mar Pet Geol 83, 246–260. https://doi.org/10.1016/j.marpetgeo.2017.03.013

Volpi V, Forlin F, Donda F, Civile D, Facchin L, Sauli S, Merson B, Sinza-Mendieta K, Shams A (2015) Southern adriatic sea as a potential area for CO2 geological storage. Oil Gas Sci Technol 70, 713–728. https://doi.org/10.2516/ogst/2014039

Yilmaz Ö (2001) Seismic data analysis: processing, inversion, and interpretation of seismic data. Doherty S.M.(ed), Investigation in Geophysics, Society of Exploration Geophysicists, Tulsa, Oklahoma, USA

Figure captions

Fig 1 (a) Structural sketch map showing the remnant of Adria surrounded by Alps, Apennines (within the Italian Peninsula) and Dinarides-Albanides-Hellenides orogenic belts (modified after Cicala et al., 2021); Basemap after Google Earth Pro (2021). (b) Map of the Apulia and surrounding (see Fig. 1a for the location) showing the seismic profiles the exploration wells provided of sonic logs falling within the B, D and F Marine Zones (ViDEPI, 2021); basemap after Google Earth Pro (2021). (c) Schematic geological cross section from the Apennines foredeep to the Dinarides-Albanides foredeep (redrawn and simplified after Fantoni and Franciosi, 2010); interval velocities (Vi) estimated by available sonic logs of the exploration wells Sabrina-1, Simona-1, Cristina-1, Branzino-1, Famoso-1, Chiara-1, Grazia-1, Grifone-1, Medusa-1, Giove-1-2 and Sparviero-1 bis (see Fig. 1b for the location) (ViDEPI, 2021)

Fig 2 Display of the possible cases (from a to h) of basic seismic pulse and polarity for a single wavelet due to abrupt acoustic impedance variation with depth; AI = Acoustic Impedance

Fig 3 Reconstructed theoretical reflectors (from a to d) expected at the abrupt increase of acoustic impedance boundary; AI = Acoustic Impedance

Fig 4 Examples of portions of seismic profiles, within the B, D and F Marine Zones surrounding Apulia (from a to e; see Fig. 1b for the location), showing the reflectors in relation to the sea water/sea floor interface. The blue arrow indicates the sea water/sea floor interface

Fig 5 Reconstructed theoretical reflectors (from a to d) expected at the abrupt decrease of acoustic impedance boundary; AI = Acoustic Impedance

Fig 6 Contact between Plio-Pleistocene clay-dominated interval, above, and Oligo-Miocene succession mainly composed of calcarenites, detected by the Giove1-2 exploration wells; the interval transit time Δt, graphically obtained as average value from the sonic log, is pointed by the arrows for both the Plio-Pleistocene and Oligo-Miocene intervals; the sonic log indicates an abrupt increase of interval velocity with the depth on the contact

Fig 7 Examples of portions of seismic profiles correlated with lithostratigraphic log of exploration wells, falling within the B, D and F Marine Zones surrounding Apulia (from a to e; see Fig. 1b for the location), showing the major reflections related to interval velocity (m/s) abrupt increases with depth (m) at lithostratigraphic successions interface

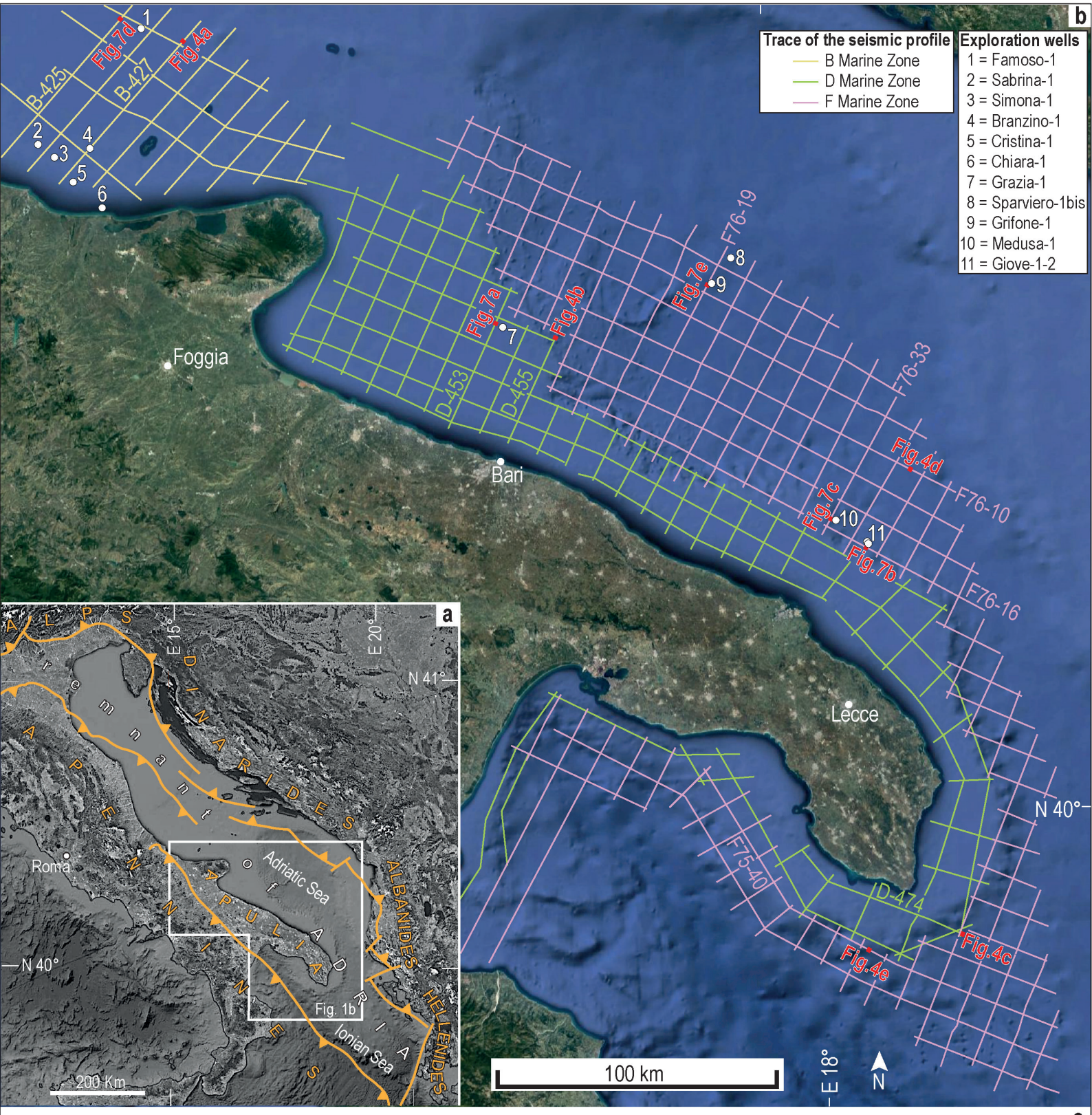
b
Trace of the seismic profile
B Marine Zone
D Marine Zone
F Marine Zone
Exploration wells
1 = Famoso-1
2 = Sabrina-1
3 = Simona-1
4 = Branzino-1
5 = Cristina-1
6 = Chiara-1
7 = Grazia-1
8 = Sparviero-1bis
9 = Grifone-1
10 = Medusa-1
11 = Giove-1-2
B-425
B-427
Fig.7d
Fig.4a
Fig.7a
Fig.4b
Fig.7e
F76-19
F76-33
Fig.4d
F76-10
Fig.7c
Fig.7b
F76-16
D-453
D-455
Foggia
Bari
Lecce
N 40°
F75-40
D-474
Fig.4e
Fig.4c
E 18°
N
100 km
a
A L P S
E 15°
E 20°
N 41°
D I N A R I D E S
Tremanti fault
A P E N N I N E S
Roma
N 40°
Adriatic Sea
of
A P U L I A
Fig. 1b
ALBANIDES
HELLENIDES
Ionian Sea
200 Km
c
km
SW
NE
0
-5
-10
A p u l i a P l a t f o r m
Bari
100 km
clays of the Apennines and Dinarides-Albanides foredeeps; Vi = 1900 - 2400 m/s, exceptionally 1650 m/s (Plio-Quaternary)
gypsum rocks of the Gessoso-Solfifera Fm; Vi = 4800 m/s (Messinian)
marls, marly limestones and calcarenites of the Dinarides-Albanides foredeep; Vi = 2400 - 3900 m/s, exceptionally 4500 m/s (Oligo-Miocene)
basin cherty limestones; Vi = 4900 - 6350 m/s (Mesozoic - Eocene)
platform limestones, e.g. Apulia Platform; Vi = 4900 - 6350 m/s (Mesozoic - Eocene)

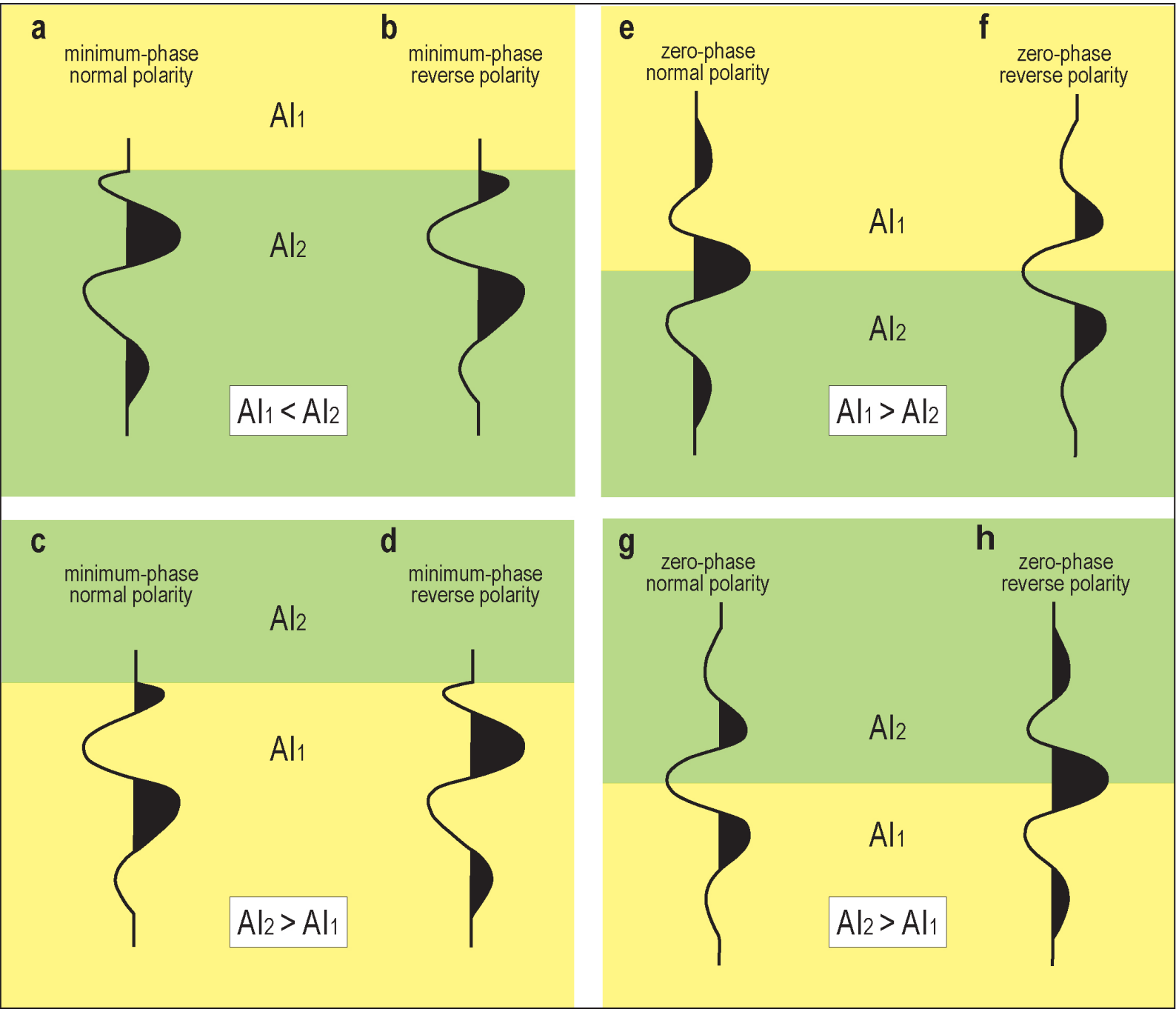
a
minimum-phase
normal polarity
b
minimum-phase
reverse polarity
Al1
Al2
Al1 < Al2
e
zero-phase
normal polarity
f
zero-phase
reverse polarity
Al1
Al2
Al1 > Al2
c
minimum-phase
normal polarity
d
minimum-phase
reverse polarity
Al2
Al1
Al2 > Al1
g
zero-phase
normal polarity
h
zero-phase
reverse polarity
Al2
Al1
Al2 > Al1

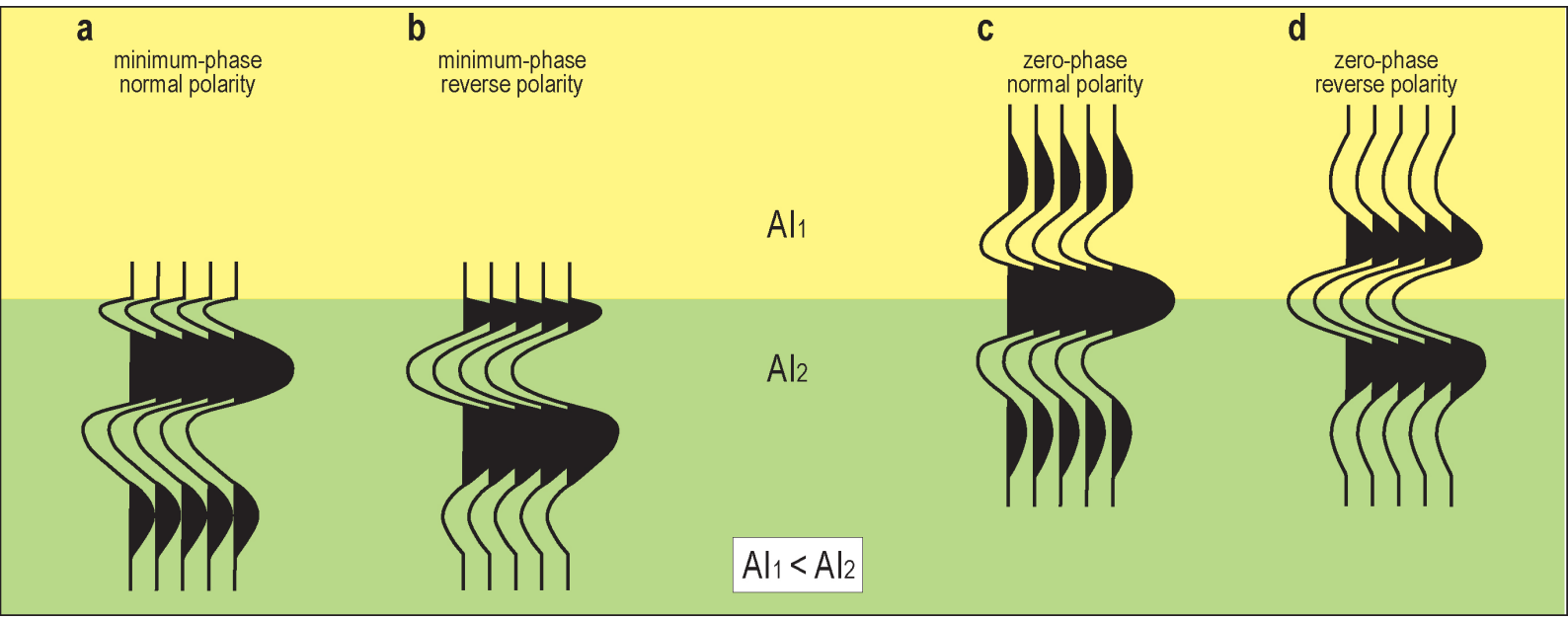
a
minimum-phase
normal polarity
b
minimum-phase
reverse polarity
c
zero-phase
normal polarity
d
zero-phase
reverse polarity
AI1
AI2
AI1 < AI2

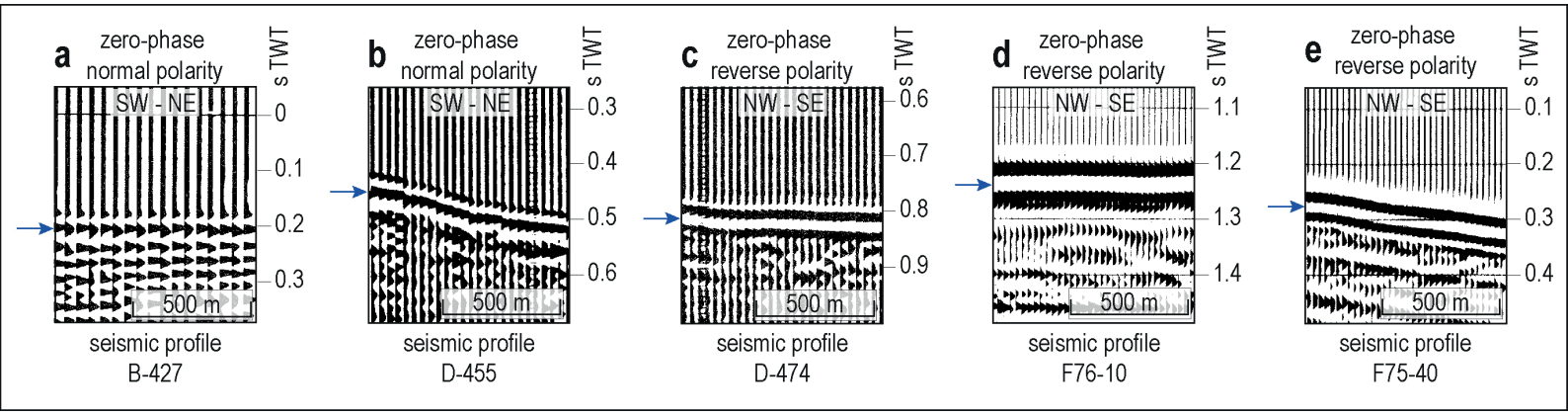
a
zero-phase
normal polarity
SW - NE
s TWT
0
0.1
0.2
0.3
500 m
seismic profile
B-427
b
zero-phase
normal polarity
SW - NE
s TWT
0.3
0.4
0.5
0.6
500 m
seismic profile
D-455
c
zero-phase
reverse polarity
NW - SE
s TWT
0.6
0.7
0.8
0.9
500 m
seismic profile
D-474
d
zero-phase
reverse polarity
NW - SE
s TWT
1.1
1.2
1.3
1.4
500 m
seismic profile
F76-10
e
zero-phase
reverse polarity
NW - SE
s TWT
0.1
0.2
0.3
0.4
500 m
seismic profile
F75-40

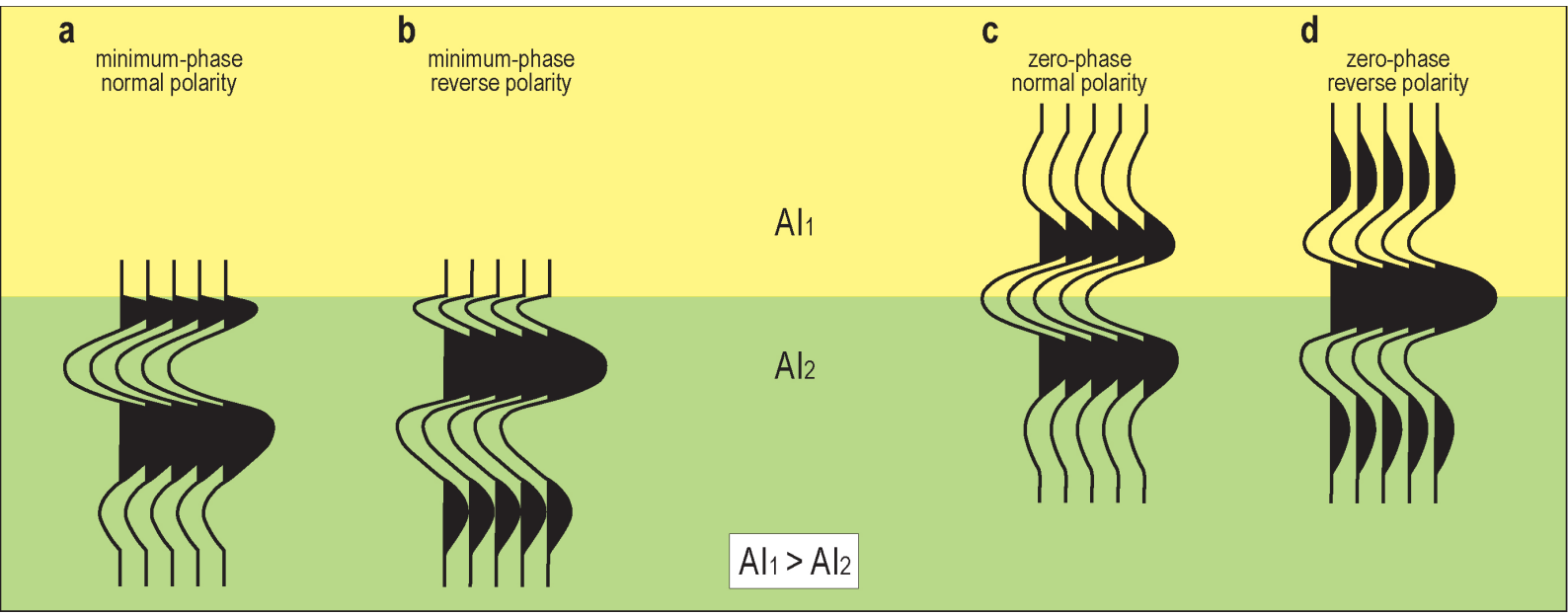
a
minimum-phase
normal polarity
b
minimum-phase
reverse polarity
c
zero-phase
normal polarity
d
zero-phase
reverse polarity
AI1
AI2
AI1 > AI2

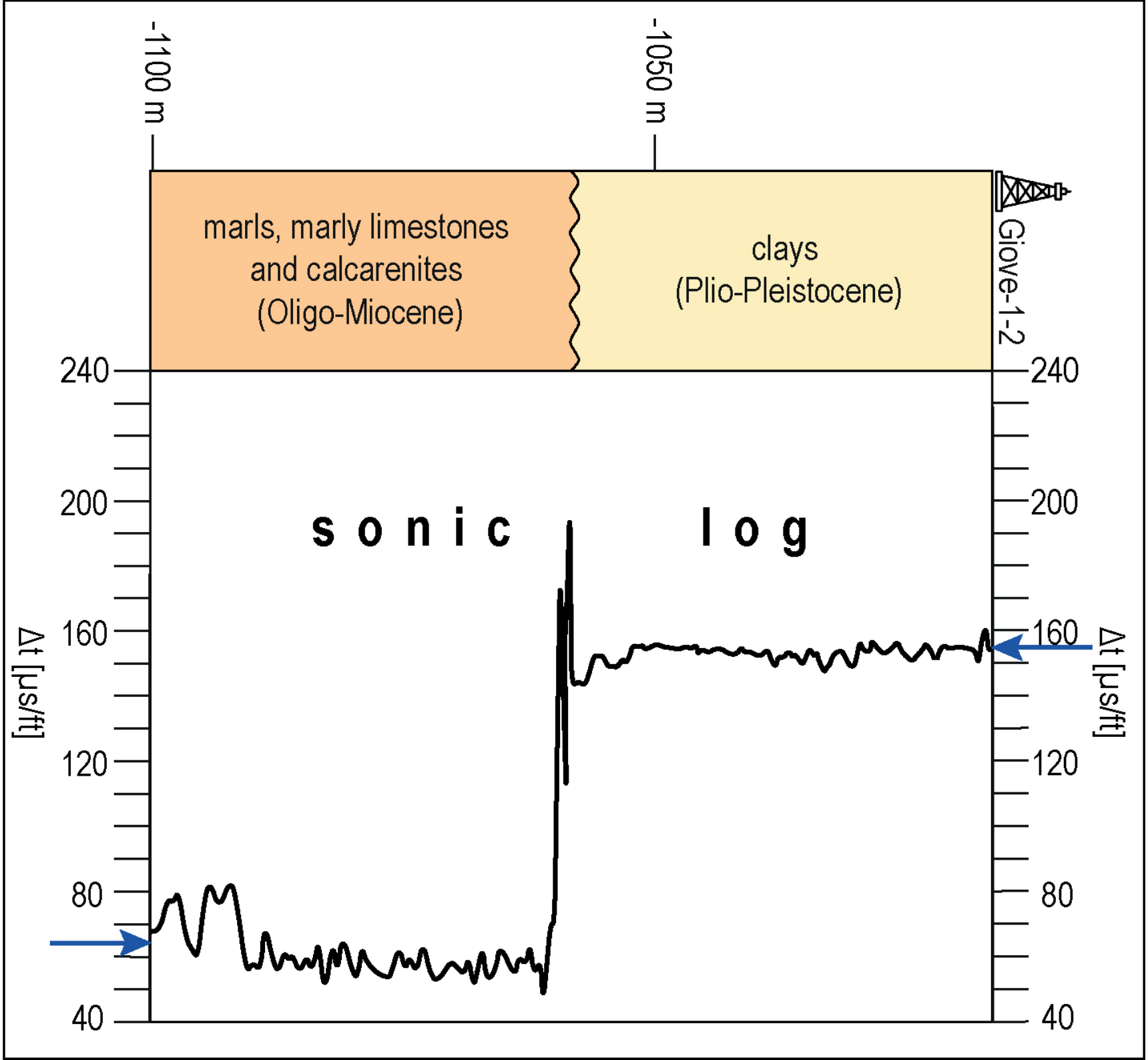
-1100 m
-1050 m
marls, marly limestones
and calcarenites
(Oligo-Miocene)
clays
(Plio-Pleistocene)
Giove-1-2
240
200
160
120
80
40
sonic log
Δt [μs/ft]
Δt [μs/ft]

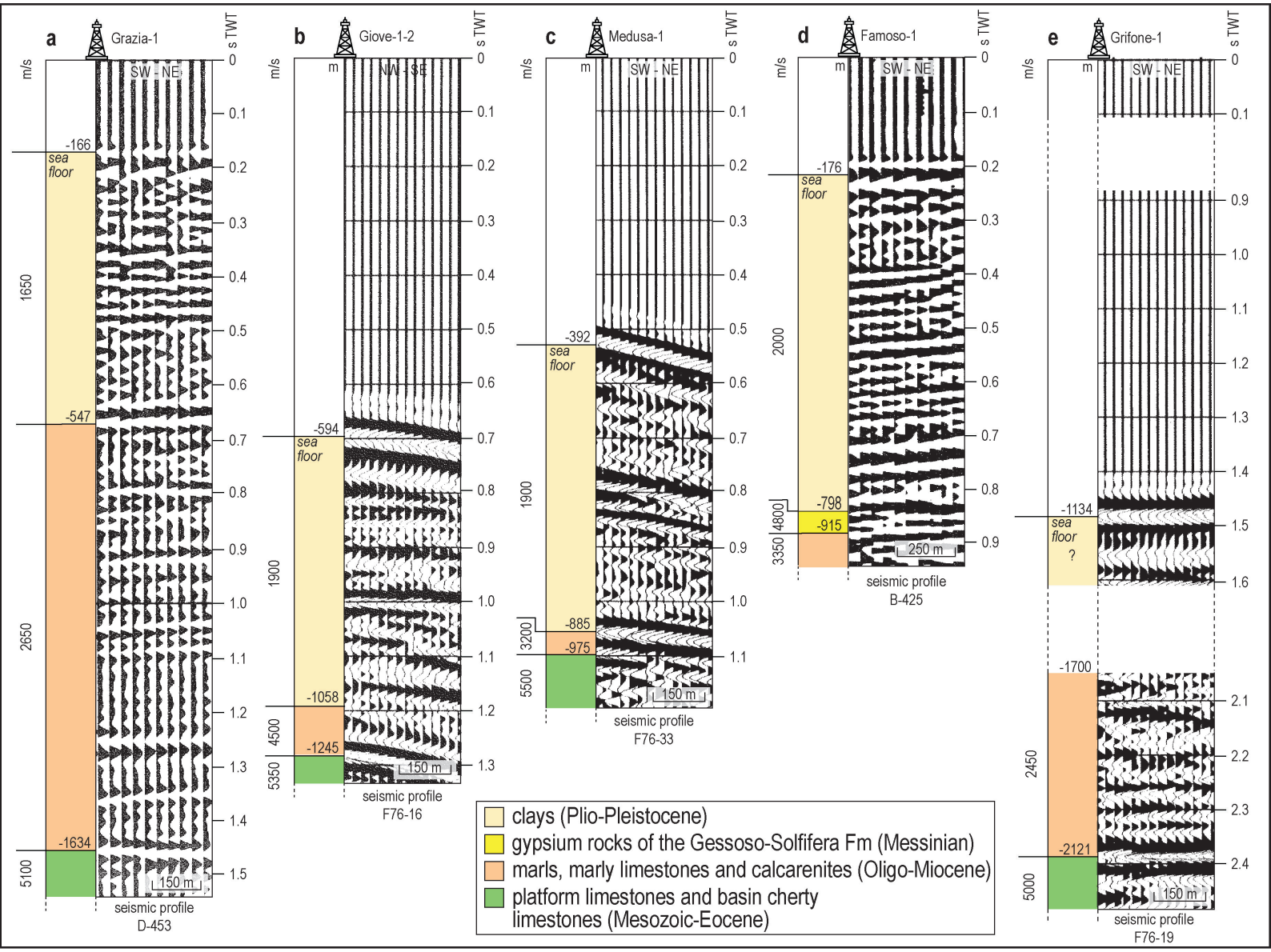
a
Grazia-1
m/s
s TWT
SW - NE
-166
sea floor
1650
-547
2650
-1634
5100
150 m
seismic profile
D-453
b
Giove-1-2
m
NW - SE
-594
sea floor
1900
-1058
4500
-1245
5350
150 m
seismic profile
F76-16
c
Medusa-1
m
SW - NE
-392
sea floor
1900
-885
3200
-975
5500
150 m
seismic profile
F76-33
d
Famoso-1
m
SW - NE
-176
sea floor
2000
-798
4800
-915
3350
250 m
seismic profile
B-425
e
Grifone-1
m
SW - NE
-1134
sea floor ?
-1700
2450
-2121
5000
150 m
seismic profile
F76-19
clays (Plio-Pleistocene)
gypsium rocks of the Gessoso-Solfifera Fm (Messinian)
marls, marly limestones and calcarenites (Oligo-Miocene)
platform limestones and basin cherty limestones (Mesozoic-Eocene)